Cancer Chemotherapy in Early Life Significantly Alters the Maturation of Pain Processing

G. J. Hathway, [b]* Emily Murphy, [a] Joseph Lloyd, [b] Charles Greenspon [b] and R. P. Hulse [a,c]*

[a] *Cancer Biology, School of Medicine, University of Nottingham, Nottingham NG7 2UH, United Kingdom*

[b] *School of Life Sciences, University of Nottingham, Nottingham NG7 2UH, United Kingdom*

[c] *School of Science and Technology, Nottingham Trent University, Clifton Lane, Nottingham NG11 8NS, United Kingdom*

Abstract—Advances in pediatric cancer treatment have led to a ten year survival rate greater than 75%. Platinum-based chemotherapies (e.g. cisplatin) induce peripheral sensory neuropathy in adult and pediatric cancer patients. The period from birth through to adulthood represents a period of maturation within nociceptive systems. Here we investigated how cisplatin impacts upon postnatal maturation of nociceptive systems. Neonatal Wistar rats (Postnatal day (P) 7) were injected (i.p.) daily with either vehicle (PBS) or cisplatin (1mg/kg) for five consecutive days. Neither group developed mechanical or thermal hypersensitivity immediately during or after treatment. At P22 the cisplatin group developed mechanical ($P < 0.05$) and thermal ($P < 0.0001$) hypersensitivity versus vehicle group. Total DRG or dorsal horn neuronal number did not differ at P45, however there was an increase in intraepidermal nerve fiber density in cisplatin-treated animals at this age. The percentage of IB_4+ve, CGRP+ve and NF200+ve DRG neurons was not different between groups at P45. There was an increase in TrkA +ve DRG neurons in the cisplatin group at P45, in addition to increased TrkA, NF200 and vGLUT2 immunoreactivity in the lumbar dorsal horn versus controls. These data highlight the impact pediatric cancer chemotherapy has upon the maturation of pain pathways and later life pain experience.

This article is part of a Special Issue entitled: SI: Pain Circuits. Crown Copyright © 2017 Published by Elsevier Ltd on behalf of IBRO. This is an open access article under the CC BY license (http://creativecommons.org/licenses/by/4.0/).

Key words: cisplatin, neuropathy, pain, hyperalgesia, development, postnatal.

INTRODUCTION

Platinum-based chemotherapies (e.g. oxaliplatin, cisplatin) are front line cancer treatments (van As et al., 2012). However, these cytotoxic drugs not only target cancerous cells but also other non-cancerous cell types and thus produce considerable side-effects. Up to 95% of adult patients suffer from sensory complications (e.g. pain, numbness) during or following chemotherapy, which typically affect the extremities (hands and feet) (Paice, 2011; Giles et al., 2007). Consequently chemotherapy-induced sensory neuropathies (CIPN) can impede success of treatment and in some cases lead to treatment being terminated (Park et al., 2013). Many adult-patients suffer CIPN after initial cisplatin exposure (McWhinney et al., 2009), which can persist for many months following cessation of treatment (Seretny et al., 2014). Cisplatin-induced CIPN has been investigated extensively in rodent models (Joseph and Levine, 2009; Uhelski et al., 2015) with translatable hallmarks of sensory neuropathy presented such as sensory neuron degeneration (intraepidermal sensory nerve fiber (IENF) innervation loss and axonal degeneration) (Ta et al., 2006; Mao-Ying et al., 2014) and sensory neuron hyperexcitability (Joseph and Levine, 2009; Uhelski et al., 2015).

Despite the significant implications for adult cancer survivors, understanding the impact of chemotherapy-induced sensory neurotoxicity upon childhood cancer survivors has not been extensively investigated. Against a background of increased cancer patient survival rates in the general population, improvements in treating pediatric cancer has resulted in survival rates of ∼75% surviving longer than 5–10 years (Smith et al., 2010; Ward et al., 2014). Pediatric cancer treatments are similarly invasive to that in adults, with highly cytotoxic agents administered and surgical interventions often required. Evidence exists to show that chemotherapy treatment early in life leads to a significant decline in quality of life in adult childhood cancer survivors. Typically many patients complain of fatigue, anxiety and depression (Clanton et al., 2011; Kunin-Batson et al., 2016) as well as impairment of the auditory system that significantly

effects social interactions and cognitive development (Grewal et al., 2010). However, exposure to chemotherapy at a young age leads to pain (Lu et al., 2011), especially in the extremities (hands, arms) Lu et al., 2011; Gilchrist et al., 2014 and alterations in sensory function (Ness et al., 2013). This pain manifests itself in adulthood many years after diagnosis and discontinuation of treatment (Ness et al., 2013; Khan et al., 2014; Phillips et al., 2015). Cisplatin is a commonly utilized chemotherapeutic agent used in pediatric oncology, for example in treating hepatoblastoma (Zsiros et al., 2010; Zsiros et al., 2013) and studies investigating neuropathy in survivors demonstrate that cisplatin treatment early in life leads to the develop of pain in adulthood in these patients (Gilchrist and Tanner, 2013; Gilchrist et al., 2014). However, there has currently been no investigation into the mechanistic avenues by which cisplatin induces pain in childhood cancer survivors.

Nociceptive pathways are not fully developed at birth and maturation of the sensory nervous system during early life is greatly manipulated by disease and injury (Fitzgerald, 2005). During infancy the peripheral nervous system is still developing. The central terminals of primary afferent sensory neurons are still to be 'hard wired' and physiological properties of dorsal horn networks that are activated by these afferents are also immature. Nerve injury early in life has been shown to result in a pronounced hyperalgesia that emerges in adulthood (Vega-Avelaira et al., 2012; McKelvey et al., 2015). This study was designed to determine whether cisplatin treatment early in life leads to an alteration in pain perception in adulthood. In Sprague–Dawley rats we report alterations in behavioral pain thresholds following cessation of treatment that persisted into adulthood, which is accompanied by changes in the classification of dorsal root ganglia (DRG) sensory neurons and alterations in sensory nerve fiber termination in the skin and spinal dorsal horn (DH).

EXPERIMENTAL PROCEDURES

Animals

Time mated pregnant Wistar rat dams were bought from Charles River UK, They were received into The University of Nottingham Biological Services Unit at E17 and allowed to habituate prior to partuition. Experiments were conducted under UK Home Office regulations and in concordance with the Animal (Scientific Procedures) Act (1986) and adhered to the ARRIVE Guidelines. Ethical approval was granted by the University of Nottingham Animal Welfare and Ethical Review Board. Animals were housed in light/dark (12:12 h) cycled rooms. Pups were housed with their mother and littermates until P21 when they were

weaned. Post-weaning rats were housed in single-sex cages of six animals with access to food and water *ab libitum*. Experimenters were blinded to all treatment groups at all stages.

Nociceptive behavioral experiments

Pups of both genders were randomly assigned to two groups, vehicle ($n = 22$) and cisplatin ($n = 19$) at birth (Postnatal (P) 0). Animals were treated with experimental agents from P7. The vehicle group were administered PBS (phosphate-buffered saline) and the treatment group administered cisplatin (1mg/kg dissolved in PBS) intraperitoneal (i.p.) injections once a day for five consecutive days (Fig. 1A) in two cohorts. In reference to human cisplatin administration, a single cycle of cisplatin treatment (typically between 60 and 100 mg/m^2, every ∼3 weeks (Zsiros et al., 2010), with for example hepatoblastoma patients 19.1 months old (median age) receive 70 mg/m^2/cycle patients (Zsiros et al., 2013). The dose of cisplatin used in this study is comparable to adult rodent studies which demonstrate sensory neuropathy (Park et al., 2013; Uhelski et al., 2015). One cohort was terminated at P16 (Immature) (vehicle ($n = 8$) and cisplatin ($n = 11$) the remainder remained in the study until P45 (adult). Prior to behavioral testing animals were habituated to handling and the room in which testing occurred. Mechanical withdrawal threshold and withdrawal latency to heat were measured as previously described (Vencappa et al., 2015). Mechanical threshold was measured using von Frey filaments (Linton), which were applied to the dorsal surface of the left and right hind paw of pups (< P21) or the plantar surface in older animals (> P21). Each hair (expressed in grams) was applied sequentially, five times each to determine
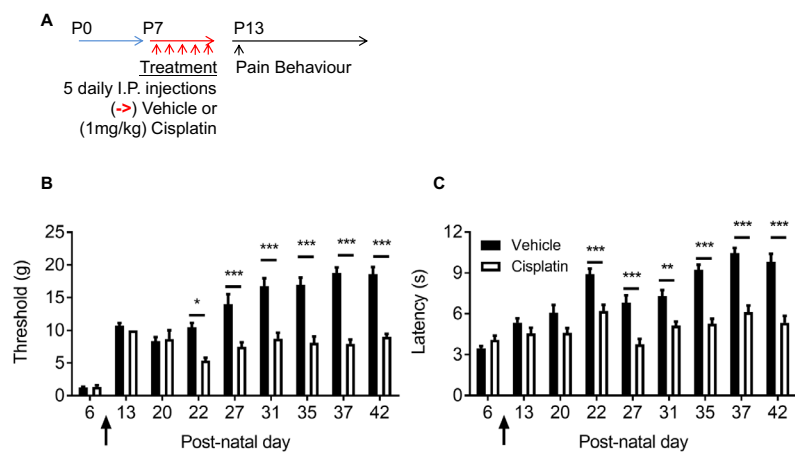
Fig. 1. Cisplatin treatment results in a delayed mechanical and thermal hypersensitivity. [A] P7 rats were treated with either i.p. injections of vehicle or cisplatin (1 mg/kg) for 5 consecutive days. [B] Experimental groups of animals did not display any alterations in mechanical withdrawal threshold between P6 and P20. However, from P22 to the end of the experiment the cisplatin-treated animals displayed a reduction in withdrawal threshold to mechanical stimulation when compared to vehicle injection ($^*P < 0.05$, $^{***}P < 0.001$ Two ANOVA with post Bonferroni test; vehicle = 7, cisplatin $n = 5$). [C] In response to heat, animals from both experimental groups demonstrated similar withdrawal latencies. At P22 cisplatin-treated animals displayed a reduction in withdrawal latency to heat stimulation ($^{**}P < 0.01$, $^{***}P < 0.001$ Two ANOVA with post Bonferroni test; vehicle = 7, cisplatin $n = 5$).

mechanical force withdrawal thresholds which was determined as the first hair to elicit a withdrawal response in 40% of applications. Latency (seconds) to withdraw from a thermal stimulus was achieved using the plantar test (Hargreaves Apparatus, Ugo Basile). Thermal stimuli were applied to both feet three times, with a rest period between stimulations to avoid sensitization and the mean latency to the three presentations calculated.

Immunohistochemistry

Animals were terminally anesthetized with sodium pentobarbital (60 mg/ml; i.p.). The heart of each animal was exposed and blood collected from the left ventricle via cardiac puncture into heparinized tubes and stored at 4 °C. Animals were then perfused transcardially via this cannula with ice-cold PBS (> 100 ml) followed by 4% paraformaldehyde (PFA; > 200 ml). Tissue (spinal cord, L3-5 dorsal root ganglia (DRG), plantar hindpaw skin-full plantar width skin biopsies were extracted from mid-point of the heel to the proximal border of the footpad (excluding footpads Thakur et al., 2012) was collected and submerged in 4% PFA and left overnight at 4 °C. Tissues were then transferred to a 30% sucrose (in Phosphate buffer saline (PBS)) solution, kept at 4 °C overnight. Samples were then frozen in optimum cutting temperature (OCT) solution and stored at −80 °C until needed. Sections were cut using a cryostat and mounted on a Superfrost Plus slides (VWR International) and stored at −80 °C. Dorsal root ganglia were cut at 6 μm, plantar skin 20-μm thickness and spinal cord 40 μm.

Slides were placed in a humidified chamber and washed with PBS solution (3 times for 5 min each) and then with PBS 0.2% Triton x-100. Slides were incubated in blocking solution (PBS 0.2% Triton x-100 5% Bovine Serum Albumin (BSA) 10% Fetal Bovine Serum (FBS)) for 30 min at room temperature. Primary antibodies were made up at required concentration in blocking solution. Antibodies, concentrations, sources are: mouse anti-NeuN (Millipore) (1 in100), Rabbit anti-protein gene product 9.5 (PGP9.5) (Millipore, 1 in200), Rabbit anti-calcitonin gene related peptide (CGRP) (Sigma, 1in 5000), mouse anti-Neurofilament 200 (NF200) (Sigma, 1 in 1000), goat anti-tropomyosin receptor kinase A (TrkA) (R&D Systems, 1 in 100), rabbit anti-cleaved caspase 3 (Cell Signalling, 1 in 500). These were incubated overnight at 4 °C. Slides were then washed a further 3 times (5 min) in PBS. In some cases biotinylated antibodies were used (biotinylated donkey anti rabbit and biotinylated donkey anti goat, Jackson, 1 in 500). These were made up in PBS 0.2% Triton x-100 was pipetted to slides and left at room temperature for 2 h. These were washed 3 times (5 min) in. Slides were then incubated in Alexafluor antibody (Invitrogen, 1 in 1000) diluted appropriately in PBS 0.2% triton x-100 and were left in a dark environment at room temperature for 2 h. Alexafluors used were anti-mouse 488, streptavidin 555, streptavidin 405, and anti-rabbit 555. These were washed 3 times (5 min) in PBS. Slides were coverslipped (22 × 50 mm) using Fluorsave (Millipore). Fluoroshield with DAPI (Millipore) was used for the plantar skin sections. Coverslips were sealed and stored

at 4 °C in the dark. Slides were imaged using a Leica SPE confocal microscope and Leica Application Suite Software (TVBL imaging facility). Each DRG section was imaged in its entirety and for the plantar skin slides 4–6 random images were taken per section to provide a representation. The x10 objective was used to image the DRGs and plantar skin sections for quantitative analysis and the x63 objective was used to generate high magnification images.

Spinal cords were cut at 40 μm using a microtome and left in sucrose azide (0.04%) overnight. Sucrose azide was removed by washing in PBS (3× for 5 min). Slides were incubated with 3% blocking solution (0.1 M PBS, 3% goat or donkey serum, 0.3% triton X-100) for one hour at room temperature. Primary antibodies, sources, concentrations and incubation times are: mouse anti NeuN (Millipore, 1 in 500), rabbit anti-GFAP (AbCam, 1 in 500, Goat anti-TrkA (R&D Systems) (1 in 100), overnight. (Donkey anti-goat biotin (1 in 500) 2 h), Mouse anti-NF200 (Sigma) (1 in 750) 24 h, Rabbit anti-VGLUT2 (Synaptic Systems) (1 in 750) 24 h. The slides were then washed in PBS 5× for 10 min. Life technologies alexafluors used were; Streptavidin 405 (1 in 1000), anti-mouse 488 (1 in 500), anti-rabbit 555 (1 in 500). Samples were incubated for 2 h at room temperature in the dark, before washing in PBS 5× for 10 min. Sections were mounted on gelatinized slides and allowed to dry overnight in the dark. Slides were coverslipped (22 × 50 mm) using Fluromount (Sigma), sealed and stored in the dark at 4 °C. Slides were imaged using a Leica SPE confocal microscope and Leica Application Suite Software (TVBL imaging facility), the dorsal horn of the spinal cord was imaged using the ×10 objective.

Analysis

Analysis was completed using Microsoft Excel and GraphPad Prism v 6.0 software. All data are presented as mean ± SEM. The area per field of view is 1.10 mm × 1.10 mm at ×10 magnification. Neuronal number and section area (μm^2) were quantified automatically using Image J software region of Interest (ROI) manager tool (http://imagej.net/Welcome). IB4^{+}, CGRP[+], TrkA[+] and NF200^{+} neurons were calculated as a percentage of the total DRG number (NeuN[+]/PGP9.5[+]stained). Total DRG neuronal number was determined from using PGP9.5 and NeuN co-staining and quantified per ROI (whole DRG section). A minimum of 10 sections per animal used and mean total sensory neuron count per DRG was determined. It was determined that the total neuronal number for PGP9.5 and NeuN was similar between treatment groups (Fig. 5). IENF density were quantified, using image J software, as fibers entering the epidermis (visualized with DAPI/dotted white line). Numbers were normalized for epidermal length (μm) and to the mean of vehicle animals. Five random images were acquired per plantar skin sample per animal with a minimum of 10 sections per animal used. From these the average IENF density score was calculated per animal. A minimum total of 7400 DRG sensory neurons and 2100 IENF were analyzed over

the complete study. All DRG and IENF analysis previously described (Hulse et al., 2015). Unpaired T test was performed on the percentage DRG number and total IENF density from plantar skin. Two-way ANOVA with post hoc Bonferroni test was performed for DRG sensory neuronal soma area analysis. Images of the spinal cords were acquired and analyzed using the region of interest/ plot profile plugin in Image J. A total of 4 random regions of interest were calculated and calibrated to depth of section. Area under the curve (AUC) analysis and an unpaired T Test were performed to determine dorsal horn innervation. Nociceptive behavioral testing was analyzed using a two-way ANOVA with post hoc Bonferroni test.

In the spinal cord stains: CGRP, IB4, TrkA, NF200 and vGLUT2 staining was analyzed by plotting four lines of interest through each image in ImageJ to measure gray value (AU) intensity using the plot profile tool. Each straight plot line (fixed width) extended ventrally 600 µm,

from the outer dorsal surface of sections/outer region of lamina I, to lamina V of the dorsal horn. The origin of each line was equally spaced following the outer curve of the dorsal horn using a similar method as previously described (Lorenzo et al., 2008). Results for each group were averaged to give a single intensity profile for cisplatin and vehicle groups. The area under the curve (AUC) was taken for the averaged intensity profile to create a figure for the entire dorsal horn. Results were tested for parametric normality with D'Agostino and Pearson omnibus normality test. Cisplatin and vehicle cell counts were compared and analyzed for statistical significance using an unpaired T-test with Kolmogorov–Smirnov post hoc test. In the spinal cord NeuN and GFAP cell counts were taken from five 100 µm × 100 µm regions of interest (ROI) for lamina I, II and V of the dorsal horn, using the ROI manager plugin on ImageJ. Results for each group, were averaged to give a single cell count for each lamina,
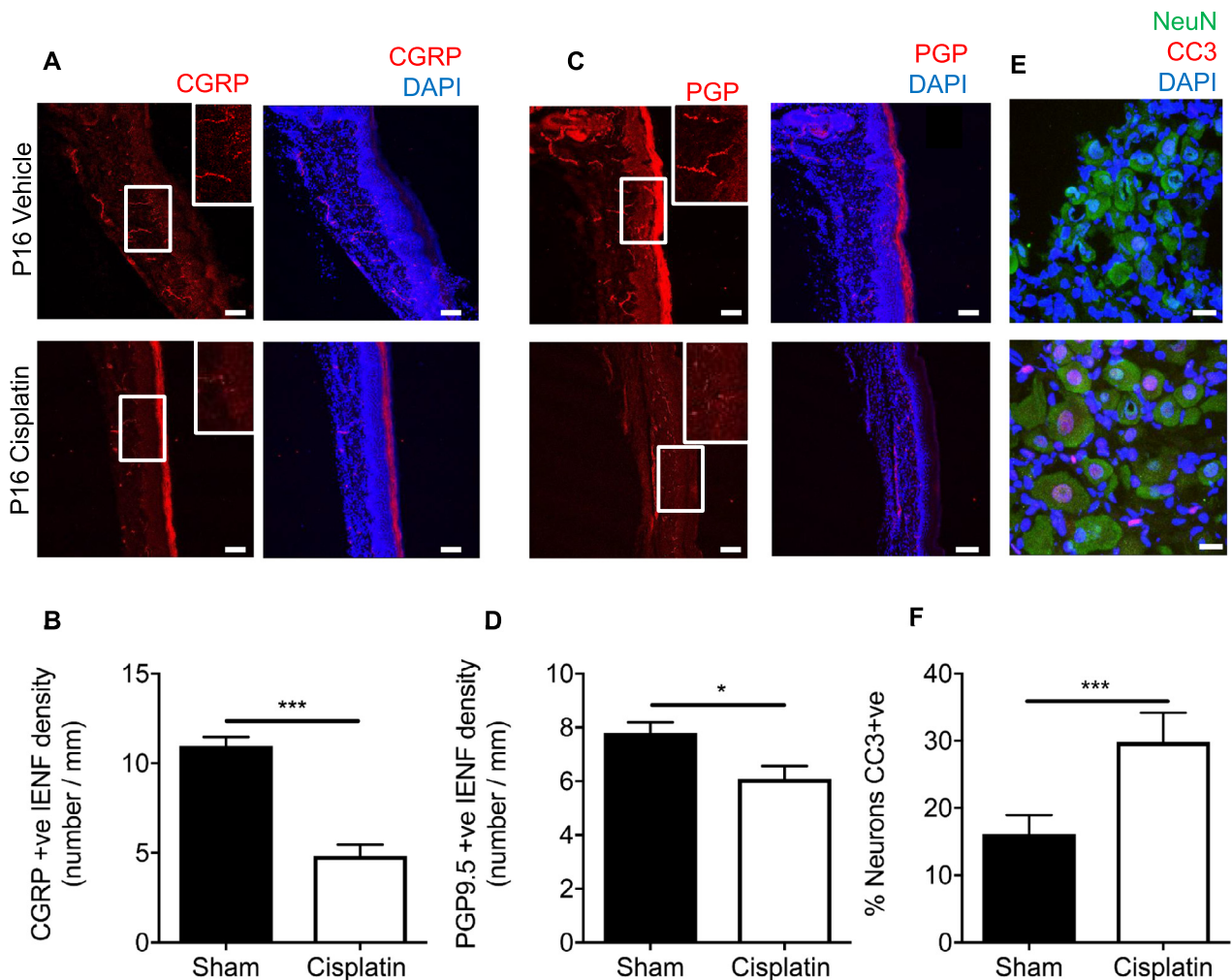
Fig. 2. Cisplatin treatment leads to sensory neurodegeneration. IENF measurements were taken from the hindpaw plantar skin from P16-20 rats treated with either vehicle or cisplatin. [A&B] There is a reduction in CGRP + ve IENF in the plantar skin of cisplatin animals versus vehicle (IENF/ mm, $^{**}P < 0.01$ Unpaired T test; vehicle = 4, cisplatin n = 4; scale bar = 100 µm). [C&D] PGP9.5 + ve IENF was also reduced in cisplatin-treated animals when compared to vehicle (IENF/mm, $^{*}P < 0.05$ Unpaired T test; vehicle = 4, cisplatin n = 4; scale bar = 100 µm). [E&F] L4 Sensory DRG neurons were collected from both experimental groups; vehicle and cisplatin at P16-20. Cleaved caspase 3 (CC3) was increased in DRG sensory neurons (NeuN + ve) in the cisplatin-treated animals versus vehicle rats ($^{*}P < 0.05$ Unpaired T test; vehicle = 4, cisplatin n = 4; scale bar = 20 µm).

and then for the entire dorsal horn section to identify total neuron or astrocyte number per dorsal horn of spinal cord and of the designated laminae. Results were tested for parametric normality with D'Agostino and Pearson omnibus normality test. Cisplatin and vehicle cell counts were compared and analyzed for statistical significance using an unpaired *T*-test with a Mann–Whitney test. *P* values are represented as *P < 0.05, **P < 0.01 and ***P < 0.001. NS dictates not significant.

RESULTS

Early-life cisplatin exposure leads to a delayed onset of mechanical and thermal hypersensitivity

To assess whether cisplatin treatment results in sensory abnormalities when administered in early-life daily intraperitoneal injections of either vehicle (PBS) or Cisplatin (1mg/kg) starting on day P7, were performed for 5 consecutive days. Cisplatin-treated animals developed a persistent but delayed (onset P22) mechanical hypersensitivity compared to vehicle-treated rats, (Fig. 1B; *P < 0.05, ***P < 0.001 Two-way ANOVA with post Bonferroni test) and this difference between the two groups was maintained until the end of the experiment (P42; Vehicle = 18.58 ± 1.09 g vs Cisplatin = 9.03 ± 0.42 g). Heat hypersensitivity also developed in the cisplatin group, with persistently shorter withdrawal latencies evident from P22 to the end of the study (P42; Vehicle = 9.82 ± 0.58 s vs Cisplatin = 5.34 ± 0.51 s) when compared to the vehicle treatment group (Fig. 1C; **P < 0.01, ***P < 0.001 Two-way ANOVA with post Bonferroni test).
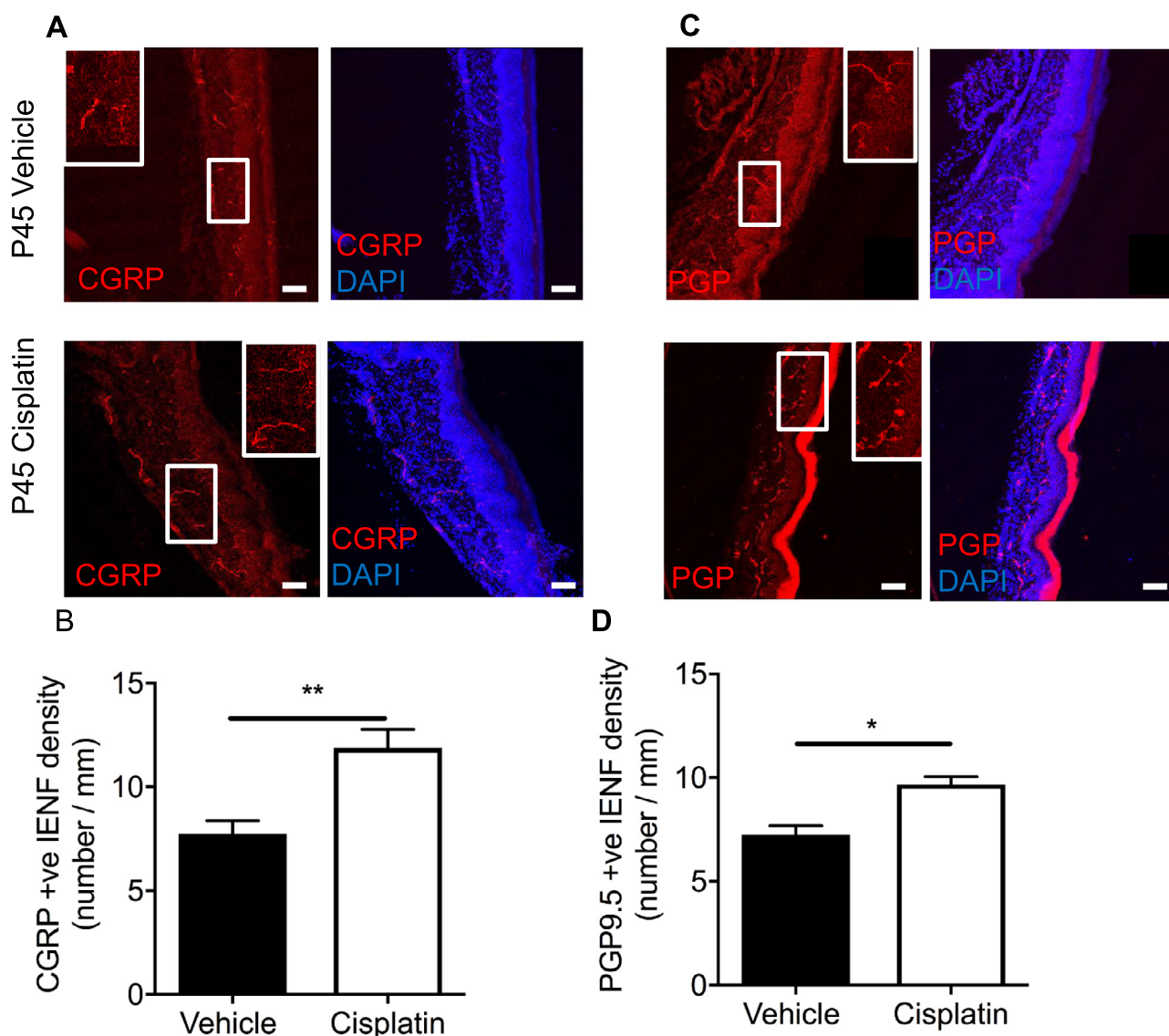
Fig. 3. Cessation of cisplatin treatment induces neuroregeneration in adults. CGRP + ve and PGP + ve IENF were measured in the plantar skin taken from hindpaws of both experimental groups; vehicle and cisplatin at P45. [A&B] In the cisplatin-treated animals there was an increase in CGRP + ve IENF versus the vehicle groups (IENF/mm, **P < 0.01 Unpaired T test; vehicle = 5, cisplatin *n* = 5). [C&D] Similarly, PGP + ve IENF was also increased in the plantar skin of cisplatin-treated animals when compared to vehicle-treated animals (IENF/mm, *P < 0.05 Unpaired T test; vehicle = 5, cisplatin *n* = 5) (scale bar = 100 μm).

Cisplatin treatment leads degeneration of the peripheral nervous system

Cisplatin is a widely used cancer chemotherapeutic, which in adults induces sensory neurodegeneration (Ta et al., 2006; Mao-Ying et al., 2014). Intraepidermal nerve fiber (IENF) density in the plantar skin and dorsal root ganglia sensory neuron number were measured in vehicle and cisplatin-treated animals a week (P16) post termination of treatment. Cisplatin exposure led to a reduction in the number of CGRP positive (Fig. 2A, B; $^{**}P < 0.01$ Unpaired T test; Vehicle = 10.98 ± 0.39 IENF/mm vs Cisplatin = 4.93 ± 1.44 IENF/mm) and PGP9.5 positive (Fig. 2C&D; $P < 0.05$ Unpaired T test; Vehicle = 7.98 ± 0.62 IENF/mm vs Cisplatin = 6.08 ± 0.32 IENF/mm) IENFs in the plantar skin versus vehicle controls. At this timepoint there were significantly more L4 DRG neurons positive for cleaved caspase 3 (CC3) in the cisplatin group when compared to vehicle animals (Fig. 2E&F; $^{**}P < 0.01$ Unpaired T test; Vehicle = $15.82 \pm 3.43\%$ vs Cisplatin = $29.89 \pm 1.49\%$). When pups were allowed to mature to P45 following treatment with cisplatin between P7-11

we observed a significant increase in the number of CGRP (Fig. 3A, B, $^{**}P < 0.01$ Un-paired T-test; Vehicle = 7.76 ± 0.62 IENF/mm vs Cisplatin = 11.88 ± 0.90 IENF/mm) positive and PGP9.5 (Fig. 3C, D, $^{*}P < 0.05$ Un-paired T-test; Vehicle = 7.25 ± 0.43 IENF/mm vs Cisplatin = 9.69 ± 0.36 IENF/mm)-positive IENF in plantar hindpaw skin compared to controls.

Cisplatin has no effect on DRG cell populations immediately following treatment

L4 DRG neurons extracted from vehicle and cisplatin-treated animals aged P16 were stained for pan-neuronal markers (Fig. 4) NeuN and PGP9.5. Sensory neurons are often categorized on the basis of their expression of neuropeptides (e.g. CGRP), lack of neuropeptides (IB$_4$) or markers of myelination (NF200). Sensory DRG neurons were labeled with (Fig. 4A) CGRP and (Fig. 4B) IB$_4$, in addition to pan-neuronal marker (Fig. 4C) NeuN. The percentage of specific sensory neuronal subsets for (Fig. 4D) CGRP (Vehicle = 53.1 ± 1.47 vs Cisplatin = 59.72 ± 2.09) and (Fig. 4E)
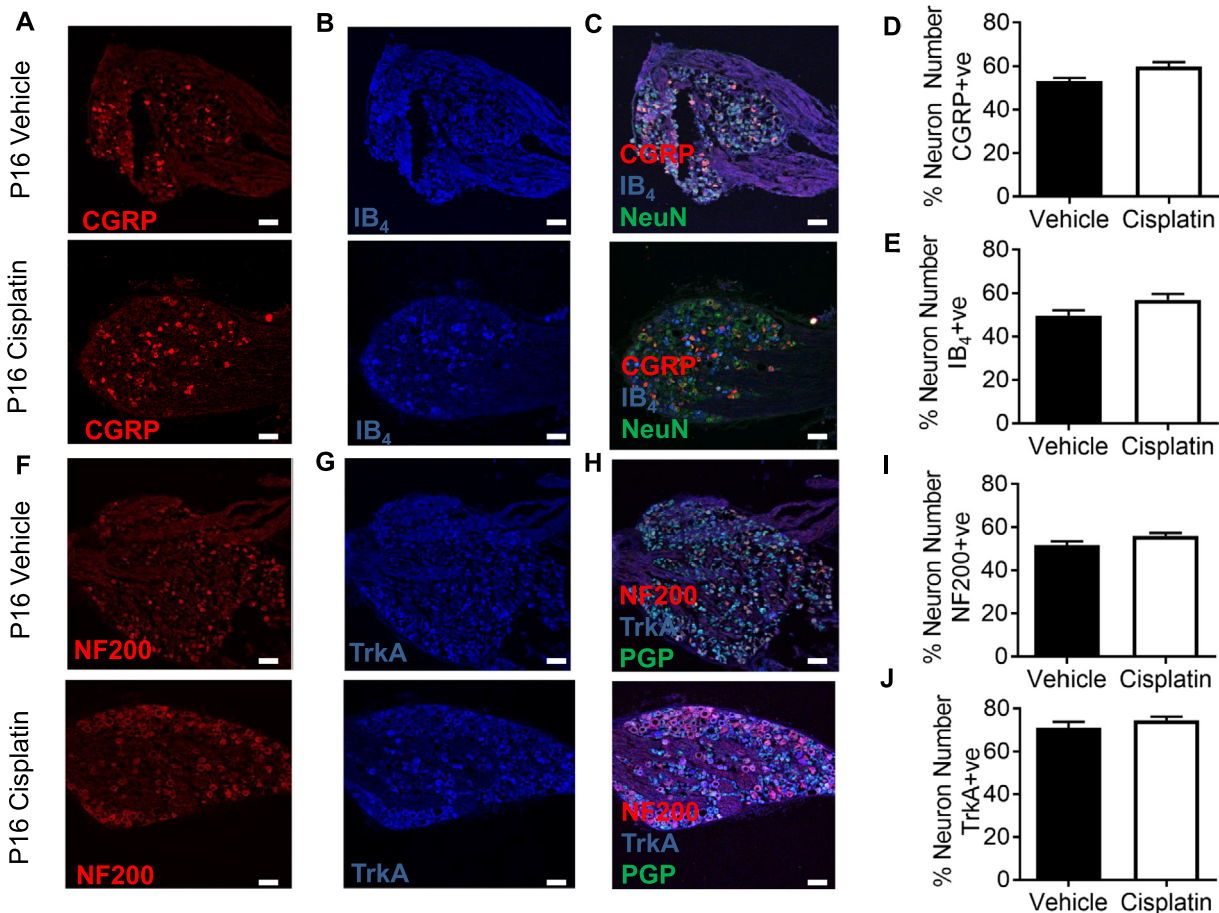
Fig. 4. Cisplatin does not alter sensory neuronal delineation. Sensory DRG neurons were stained for [A] CGRP and [B] IB$_4$ to represent the small diameter DRG sensory neuron populations in both vehicle and cisplatin-treated P16 animals. These were co-localized with [C] NeuN. There were no differences between experimental groups in the percentage of [D] CGRP and [E] IB$_4$ (non-peptidergic) sensory DRG neuronal subclasses. In addition, DRG sensory neurons were labeled for the myelinated sensory neuronal marker [F] NF200 and the small diameter neuronal marker [G] TrkA (peptidergic) in vehicle and cisplatin-treated P16 animals. These were co-localized with [H] PGP9.5. There were no differences between groups in the percentage of the [I] NF200 or [J] IB$_4$ sensory DRG neuronal subclasses (vehicle = 4, cisplatin $n = 4$; scale bar = 50 μm).

IB_4 (Vehicle = 49.53 ± 2.53% vs Cisplatin = 56.86 ± 2.63) was unchanged between experimental groups. Sensory DRG neurons extracted from age-matched vehicle and cisplatin-treated animals aged P16 were labeled with (Fig. 4F) NF200 and (Fig. 4G) TrkA, in conjunction with a pan neuronal marker, (Fig. 4H) PGP9.5. The percentage of total sensory neurons labeled with either (Fig. 4I) NF200 (Vehicle = 51.58 ± 1.85% vs Cisplatin = 55.91 ± 1.39) or (Fig. 4J) TrkA (Vehicle = 71.03 ± 2.87% vs Cisplatin = 74.53 ± 1.73) were unchanged between vehicle and cisplatin-treated groups at P16.

**Cisplatin leads to long-term re-organization of the peripheral nervous system**

We next assessed whether there were any delayed effects of neonatal cisplatin treatment upon DRG composition in rats at P45. We found that there were no significant differences in the total number of DRG sensory neurons in either experimental group at P45 (Total DRG sensory neuron number Fig. 5A, B; NeuN;

NS Unpaired T test; (Vehicle = 64.05 ± 5.19 vs Cisplatin = 67.41 ± 4.83), Fig. 5C, D; PGP9.5; NS Unpaired T test; (Vehicle = 60.59 ± 7.57 vs Cisplatin = 63.72 ± 8.01)), as well as no difference in size profiles of the DRG neurons (Fig. 5E PGP9.5 + ve; NS Two-way ANOVA with post hoc Bonferroni; NeuN size profile NS Two-way ANOVA with post hoc Bonferroni, data not shown) between experimental groups at P45. Representative images of NeuN and PGP9.5 co-localization in DRG neurons (Fig. 5F) and no primary controls (Fig. 5G; cells positive for DAPI).

At P45 the total number of sensory DRG neuronal subsets was calculated (Fig. 6A; co-labeled with NeuN) with the total number of (Fig. 6B) CGRP and (Fig. 6C) IB_4-positive neurons determined. Representative merge image of NeuN, CGRP and IB_4-positive sensory DRG neurons (Fig. 6D). There were no significant changes in the total number of CGRP + ve (Fig. 6E; NS Unpaired T test; (Vehicle = 20.83 ± 0.83 vs Cisplatin = 19.67 + 1.04%)) and IB_4 + ve (Fig. 6F; NS Unpaired T test; (Vehicle = 28.27 + 2.34 vs Cisplatin = 30.35 ± 1.15)) in either vehicle or the cisplatin-treated group.
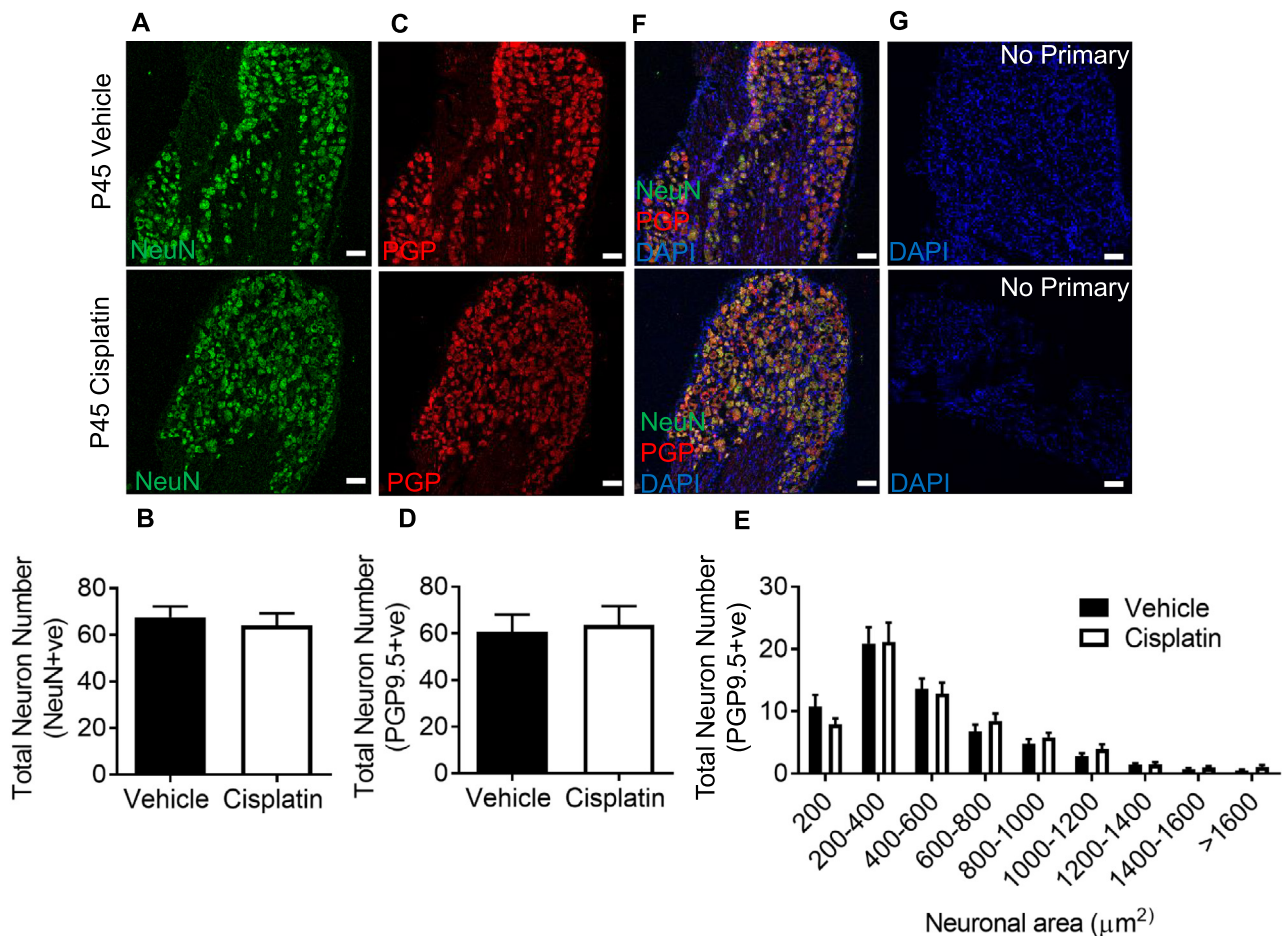
Fig. 5. The effect of cisplatin treatment on DRG sensory neurons. DRG sensory neurons were counted from both experimental groups (vehicle and cisplatin treated) at the timepoint P45. DRG neurons were stained for NeuN and PGP9.5. There was no difference in the total number of L4 DRG sensory neurons ([A–B] NeuN + ve and [C–D] PGP9.5). [E] DRG neuron size profile demonstrating no change in neuron number per designated neuronal soma area Representative image of co-staining with [F] NeuN and PGP9.5 and of [G] no primary controls (vehicle = 5, cisplatin n = 5) (scale bar = 100 μm).
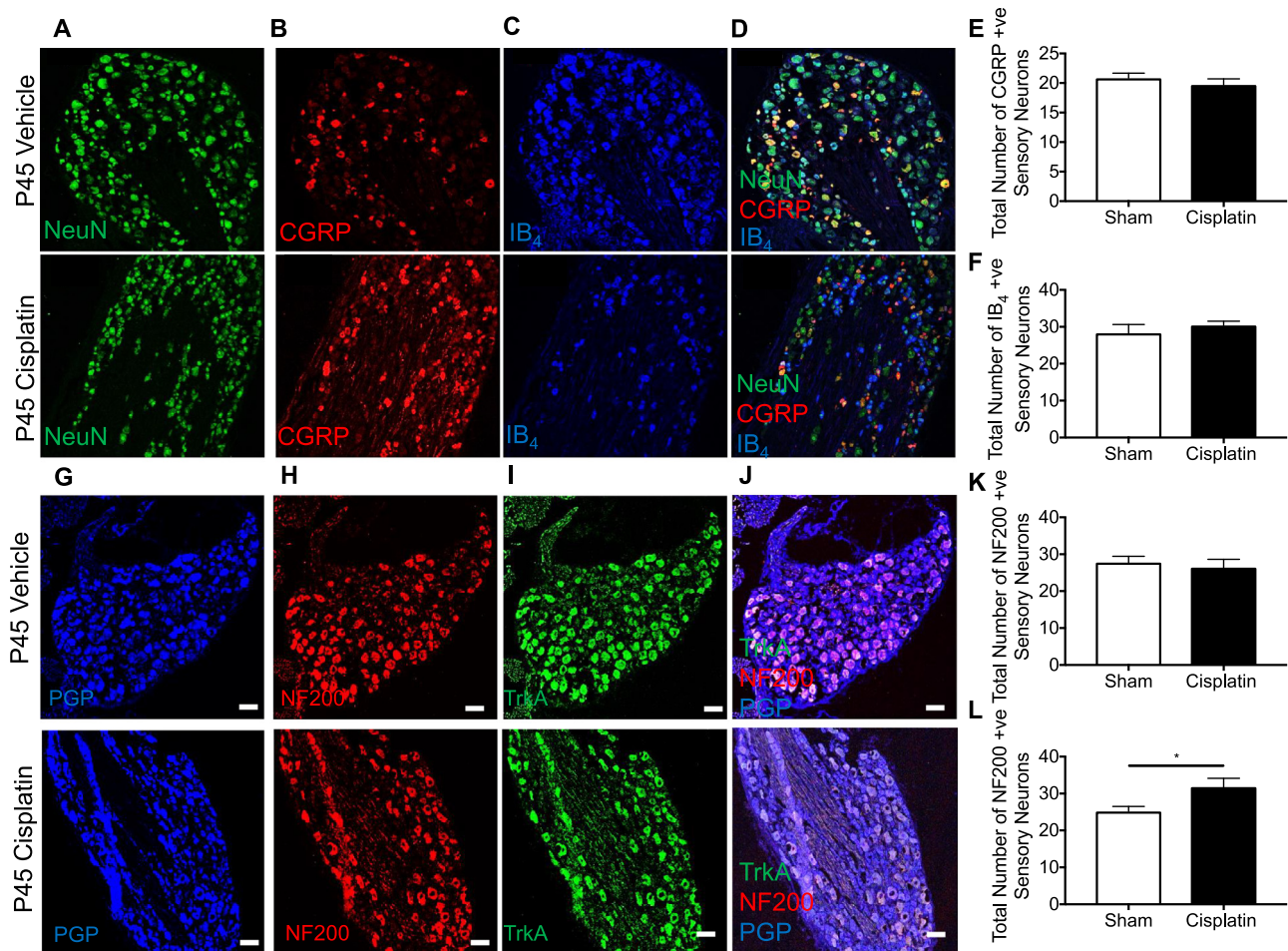
Fig. 6. The effect of cisplatin treatment on DRG neuron subclass expression in adults. Sub-classifications of L4 DRG sensory neurons were investigated in P45 animals in both vehicle and cisplatin groups. Total numbers of sensory DRG neurons were determined with [A] NeuN. Small diameter sensory DRG neurons were labeled with [B] CGRP and [C] IB$_4$. [D] Merged representation of NeuN, CGRP and IB$_4$. There were no differences between experimental groups (age-matched vehicle and cisplatin) in the total number of neurons expressing [E] CGRP or [F] IB$_4$. Total numbers of sensory DRG neurons were determined with [G] PGP9.5 when sensory DRG neurons were labeled for the myelinated sensory neuronal marker [H] NF200 and small diameter sensory neuronal marker [I] TrkA. [J] Representative image of colocalized TrkA or NF200 with PGP9.5. There were no differences between experimental groups (age-matched vehicle and cisplatin) in the total number of sensory neurons expressing [K] NF200. However, there was an increase in the percentage of DRG neurons expressing [L] TrkA in the cisplatin group ($^*P < 0.05$ Unpaired T test; vehicle = 5, cisplatin n = 5) (scale bar = 100 μm).

Furthermore, DRG sensory neurons (PGP9.5 + ve co-labeled Fig. 6G) labeled for (Fig. 6H) NF200 + ve or (Fig. 6I) TrkA (Fig. 6J; representative merge image of PGP9.5, NF200 and TrkA-positive sensory DRG neurons) demonstrated there (Fig. 6K; NS Unpaired T

test; Vehicle = 27.70 + 1.74 vs Cisplatin = 26.70 ± 2.23) was no difference between the cisplatin-treated group and the vehicle-treated group at P45 for total number of NF200-positive neurons. However, there was a significant increase in the number of TrkA + ve DRG neurons in the cisplatin group vs the vehicle group (Fig. 6L; $^*P < 0.05$ Unpaired T test; (Vehicle = 25.10 ± 1.41 vs Cisplatin = 31.76 ± 2.35) at P45. Percentage change in the sensory DRG neuron subsets are represented as a proportion of total sensory DRG neuron number (Table 1).

Early-life chemotherapy Results in immediate alterations in sensory neuron termination within the spinal dorsal horn

As well as innervating the skin, DRG neurons have a reciprocal termination with the spinal cord DH. The termination pattern of sensory neuron fibers within the

Table 1. The effect of cisplatin treatment on DRG neuron subclass expression in adults. Total number of sensory DRG neurons expressing CGRP, IB4, NF200 or TrkA were determined in experimental groups vehicle and cisplatin treat at P45 of age. ($^*P < 0.05$ Unpaired T test; vehicle = 5, cisplatin n = 5)
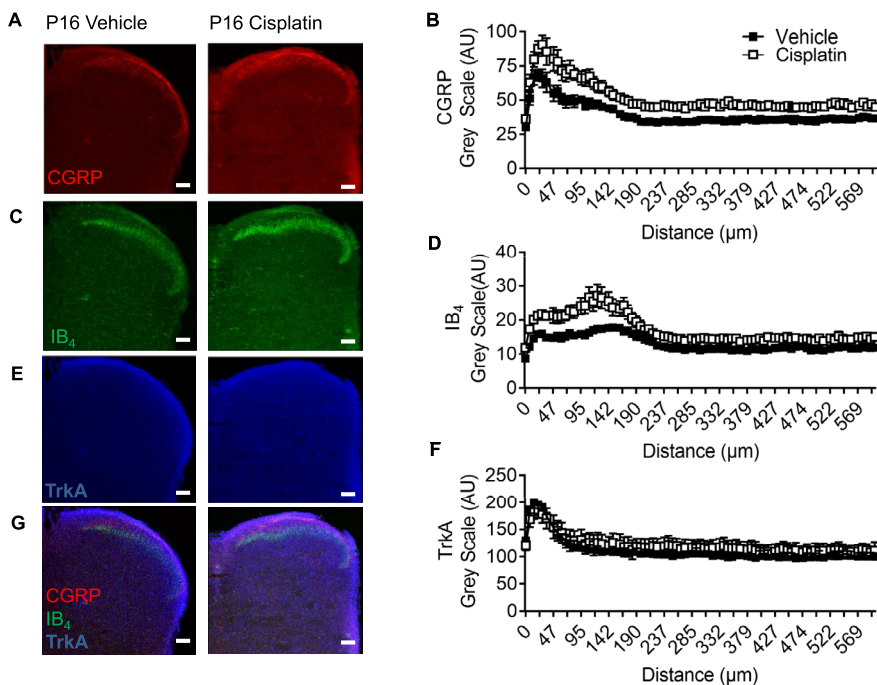
	Vehicle	Cisplatin
	% Total Sensory Neuron Number (Mean ± SEM)	% Total Sensory Neuron Number (Mean ± SEM)
CGRP	30.88 ± 1.24	30.71 ± 1.63
IB4	41.88 ± 3.46	47.39 ± 1.79
NF200	41.05 ± 2.59	41.12 ± 3.49
TrkA	37.20 ± 2.09	49.59 ± 3.67*

Fig. 7. Sensory nerve terminal innervation into dorsal horn is altered following cisplatin exposure. In cisplatin postnatal day 16 (P16) animals there was increased immunoreactivity in the superficial dorsal horn of [A-B] CGRP ($^{**}p < 0.001$ Two-way ANOVA) and [C–D] IB$_4$ ($^{**}p < 0.001$ Two-way ANOVA) compared to vehicle-treated age-matched rats. [E–F] TrkA distribution in the dorsal horn was unaltered between vehicle and cisplatin treatment groups. A merged representation of CGRP, IB$_4$ and TrkA is presented for [G] vehicle and cisplatin (vehicle = 4, cisplatin n = 4; scale bar = 100 μm).
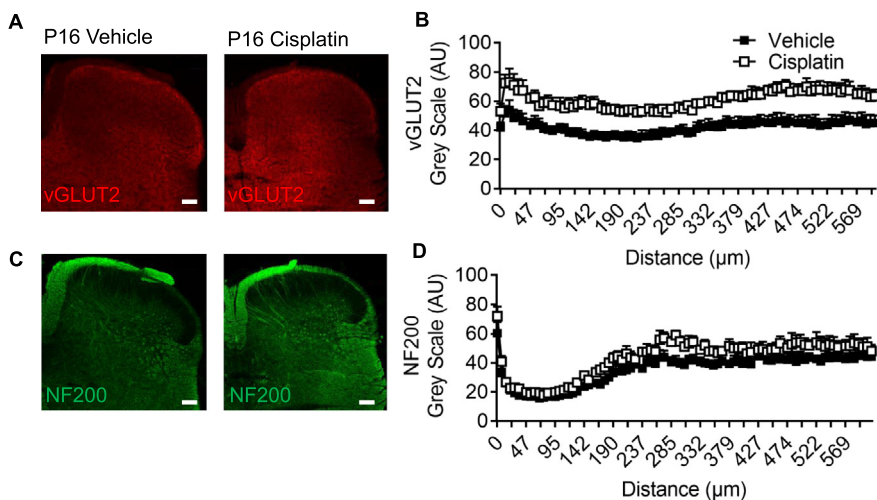
Fig. 8. Cisplatin induced reorganization of sensory nerve fiber innervation into the dorsal horn. In P16 cisplatin-treated animals [A-B] vGLUT2 sensory neuron innervation into the dorsal horn of the spinal cord was increased versus age-matched vehicle-treated rats ($^{*}p < 0.05$; Two-way ANOVA) Additionally, there was no change in [C–D] NF200 immunoreactivity between the age-matched vehicle and cisplatin-treated P16 rats (vehicle = 4, cisplatin n = 4; scale bar = 100 μm).

DH was investigated following the end of cisplatin treatment (P16) with significant differences being observed between the groups. Primary sensory nerve afferent terminals in the spinal cord were identified through immunoreactivity for CGRP, IB$_4$, and TrkA.

There was an increase in CGRP (Fig. A-7B; (Vehicle = 39.64 ± 0.53 AUC vs Cisplatin = 52.02 ± 0.74AU C) $^{**}P < 0.01$ Two-way ANOVA) and IB$_4$ (7C-D; (Vehicle = 13.08 ± 0.14 AUC vs Cisplatin = 17.22 ± 0.26AU C) $^{**}P < 0.01$ Two-way ANOVA) immunoreactivity in the dorsal horn of cisplatin animals versus age-matched vehicle controls. Whereas there was no change for TrkA (Fig. 7E, F; (Vehicle = 112.1 ± 1.42 AUC vs Cisplatin = 121.00 ± 1.07A UC)). Demonstration of colocalization and dorsal horn laminae of CGRP, IB$_4$ and TrkA in vehicle and cisplatin-treated animals (Fig. 7G). Additionally, vGLUT2 (Fig. 8A, B), which designates small diameter sensory neurons, demonstrated an increase in vGLUT2 immunoreactivity in the P16 cisplatin-treated animals (Fig. 8B; (Vehicle = 42.27 ± 0.36AUC vs Cisplatin = 61.32 ± 0.36AUC) $^{*}P < 0.05$ Two-way ANOVA). Furthermore, NF200 (Fig. 8C, D) for myelinated primary sensory nerve afferents, there was no change in NF200 (Fig. 8B; (Vehicle = 35.65 ± 0.65AU C vs Cisplatin = 43.04 ± 0.79AUC)) in the dorsal horn of cisplatin-treated animals versus vehicle controls.

At P45 sensory nerve afferent terminals in the spinal cord were identified through immunoreactivity for (Fig. 9A) CGRP, (Fig. 9B) IB$_4$, and (Fig. 9C) TrkA. CGRP sensory inputs to the DH (Fig. 9E; (Vehicle = 42.9 ± 2.61AUC vs Cisplatin = 43.65 ± 3.08AUC) NS Two-way ANOVA) was unchanged, with similar intensity and depth of innervation into the dorsal horn between vehicle and cisplatin groups. There was a small increase in IB$_4$ staining in the dorsal horn of the spinal cord of cisplatin-treated animals (Fig. 9F; (Vehicle = 23.63 ± 0.90AUC vs Cisplatin = 27.87 ± 1.25AUC) $^{*}P < 0.05$ Two-way ANOVA). There was an increase in TrkA immunoreactivity intensity and depth of innervation in the cisplatin group versus age-matched vehicle controls (Fig. 9G; (Vehicle = 53.23 ± 2.83AUC vs Cisplatin = 93.54 ± 4.46AUC) $^{**}P < 0.01$ Two-way ANOVA; representative colocalization/dorsal laminae images Fig. 9G). Furthermore, vGLUT2 (Fig. 10A-B; (Vehicle = 19.75 ± 0.17AUC vs Cisplatin = 44.01 ± 0.29AUC) $^{**}P < 0.01$
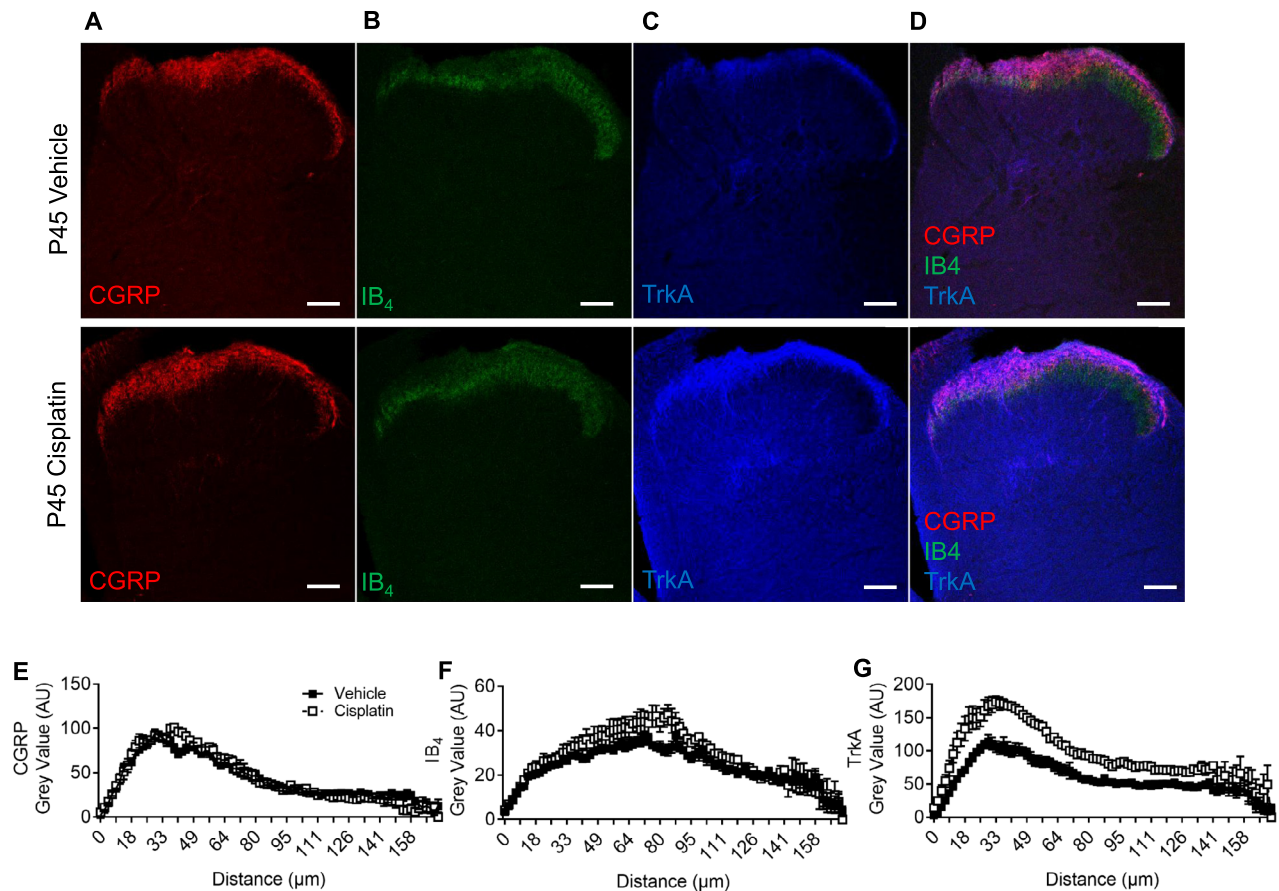
Fig. 9. Cisplatin treatment early in life leads to increased innervation of sensory afferent terminals in the superficial dorsal horn in adult rats. Sensory nerve fiber terminals within the dorsal horn of 45 day old rats (treated with either vehicle or cisplatin) were defined using [A] CGRP, [B] IB$_4$ and [C] TrkA immunoreactivity. [D] Representative overlay images of the dorsal horn displaying CGRP, IB$_4$ and TrkA nerve terminals in the vehicle and cisplatin groups. There was no change in the depth by which [E] CGRP + ve nerve fiber terminated in the dorsal and there was no change in the intensity within the dorsal horn in either experimental group (vehicle or cisplatin). [F] However, there was an increase in IB$_4$ intensity ($^*P < 0.05$ Two-way ANOVA; vehicle = 5, cisplatin $n = 5$) within the dorsal horn of cisplatin-treated animals compared to vehicle. [G] There was also an increase in intensity as well as depth of the TrkA + ve sensory nerve innervation in the dorsal horn of cisplatin-treated animals versus control. ($^{**}P < 0.01$ Two-way ANOVA; vehicle = 5, cisplatin $n = 5$). Representative merge image of CGRP, IB$_4$ and TrkA and NF200 (scale bar = 100 μm).

Two-way ANOVA) as well as NF200 (Fig. 10C-D; (Vehicle = 18.04 ± 0.43AUC vs Cisplatin = 36.2 ± 0.92AUC) $^*P < 0.05$ Two-way ANOVA; representative merge image Fig. 10E) input into the spinal cord was also increased in the cisplatin-treated animals.

Cisplatin-treated animals at P16 did not show any change in the number of NeuN-positive neuronal cell bodies (Fig. 11A–C; NS; Unpaired T test; (Vehicle = 19.18 ± 4.49 vs Cisplatin = 18.58 ± 3.98)) or GFAP expressing astrocytes (Fig. 11D-F; NS; Unpaired T test; (Vehicle = 7.08 ± 0.19 vs Cisplatin = 6.79 ± 0.32)) in the dorsal horn when compared to age-matched vehicle controls. At P45 cisplatin-treated animals did not show any change in neuron number (NeuN) (Fig. 11G–I; NS; Unpaired T test; (Vehicle = 16.8 ± 3.60 vs Cisplatin = 17.72 ± 3.46)) or astrocyte number (GFAP) (Fig. 11 J-K; NS; Unpaired T test; (Vehicle = 2.88 ± 0.38 vs Cisplatin = 3.18 ± 0.23)) at P45 across the entire spinal cord DH. However, in lamina V of the DH there was a significant increase in astrocyte expression of GFAP in cisplatin-treated adult rats (Fig. 11L; $P < 0.01$; Unpaired T test).

DISCUSSION

Chemotherapy is crucial for the treatment of cancer. Improvements in basic research, diagnosis and the advancement of anti-cancer strategies, have led to a considerable improvement in cancer survival rates. However, as a consequence of this patients and families are commonly expected to deal with the adverse long-lasting side effects of treatment. Platinum-based drugs are widely used to treat cancers and are commonly associated with sensory neuropathy in adult patients. Unfortunately, many childhood cancers are also treated with such cytotoxic agents and they can have a devastating impact upon the development of the patient. Although side-effects of treatment are well recognized (e.g. difficulties in learning and social interactions, hearing and vision (Grewal et al., 2010; Clanton et al.,
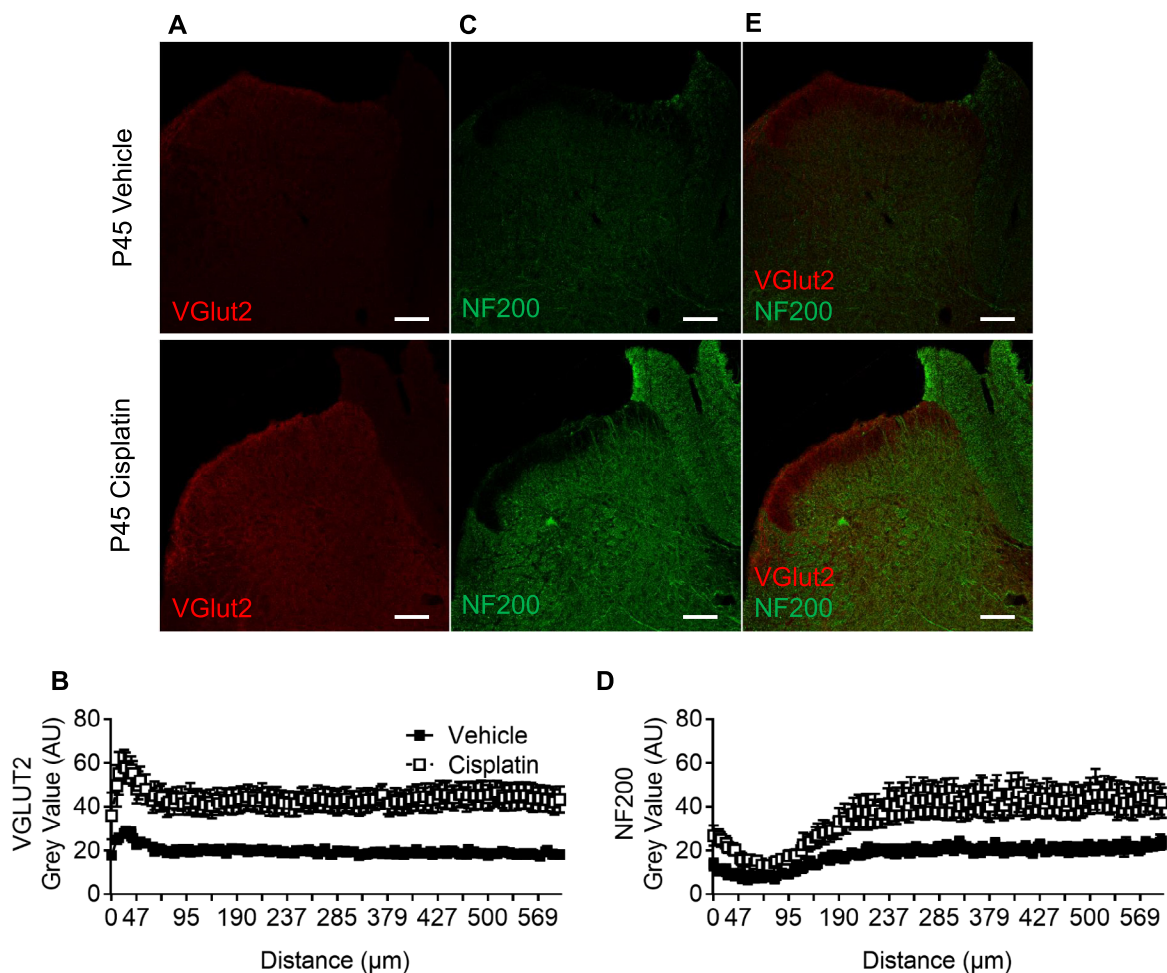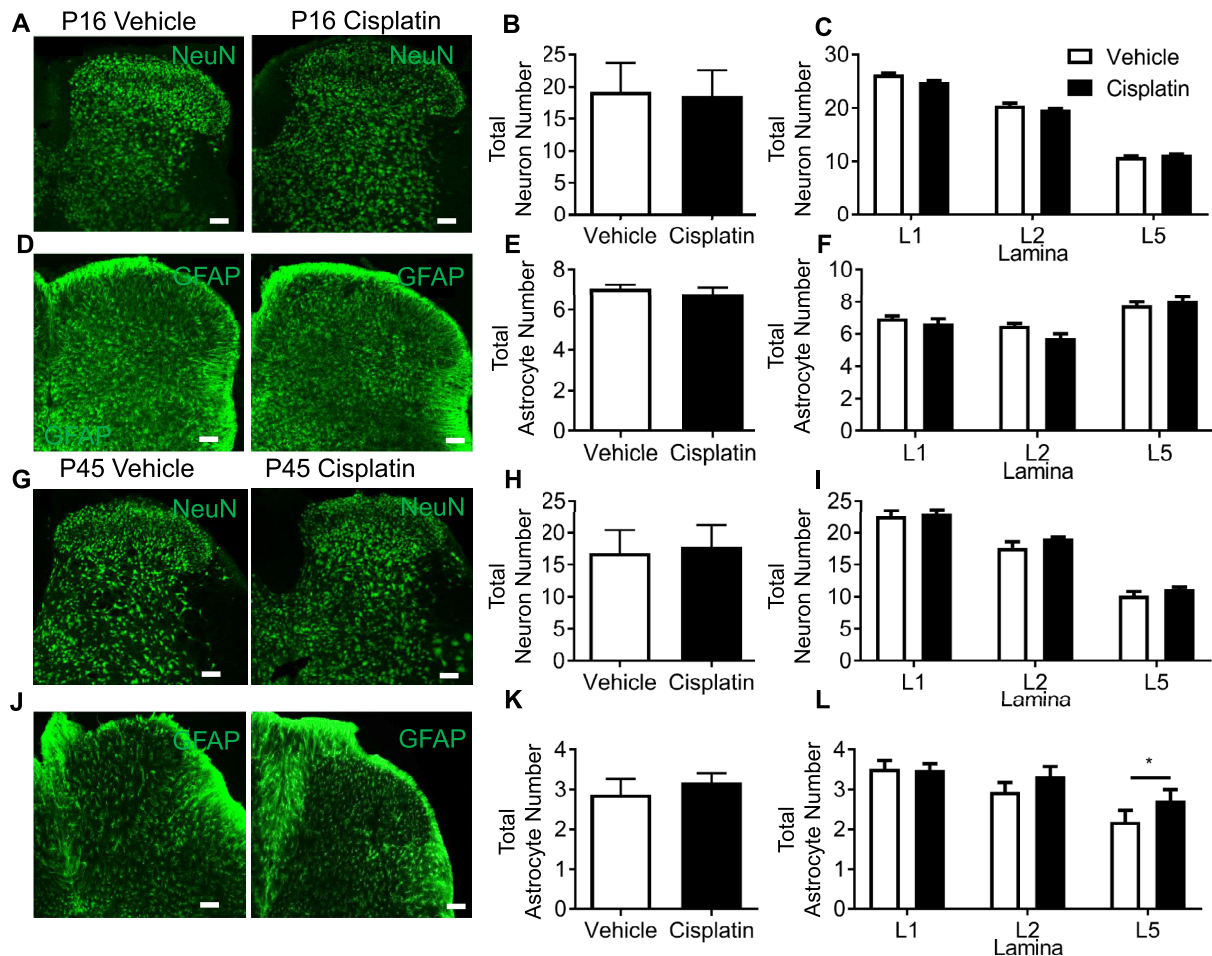
Fig. 10. Cisplatin treatment early in life leads to increased innervation of sensory afferent terminals in the superficial and deep dorsal horn in adult rats. [A] vGLUT2 + ve sensory afferent nerve terminals were found to terminate in the superficial lamina (lamina I) in the vehicle group. However, [B] there is a wide spread increase in the cisplatin group when compared to vehicle animals ([**]$P < 0.01$ Two-way ANOVA; vehicle = 5, cisplatin $n = 5$). [C] NF200 immunoreactivity demonstrates [D] an increase in myelinated structures within the dorsal horn of the spinal cord of cisplatin animals versus the vehicle group ([*]$P < 0.05$ Two-way ANOVA; vehicle = 5, cisplatin $n = 5$). [E] Representative merge image of VGlut2 and NF200 (scale bar = 100 μm).

2011), there has been minimal investigation into the impact that early-life exposure to chemotherapy has upon somatosensory development. Here we have investigated the effects of cisplatin treatment in young rodents and upon the maturing nociceptive systems in the periphery nervous system and dorsal horn of the spinal cord. Our data show that early-life cisplatin treatment leads to a delayed but prolonged pain hypersensitivity that is associated with a remodeling of the sensory nervous systems.

Cisplatin induced pain in adult childhood cancer survivors

CIPN is one of the most common side-effects and can be a treatment terminating ailment. The DRG sensory neurons are damaged by chemotherapy and a number of rodent studies have investigated this in the adult whereby mitochondrial dysfunction (Flatters and Bennett, 2006; Jin et al., 2008) and/or hindered growth factor support (Vencappa et al., 2015) are primary causes

of CIPN. However, despite the extensive research in humans and rodents to investigate adult CIPN, to date minimal research has been undertaken to investigate childhood cancers and the consequent treatment effects on quality of life. Childhood cancers are rare, however the 10-year survival rate for children surviving cancer is 75–80%. Therefore it is a clinical and moral necessity that the quality of life for these cancer survivors needs to be considered, especially as these pediatric patients are still undergoing significant bodily development. It is reported that ~50% of 10,397 adult childhood cancer survivors highlight pain as a side-effect of treatment (Lu et al., 2011), and many are dependent on prescribed analgesia medication (Lu et al., 2011). Childhood cancer patients who have undergone chemotherapy (e.g. vincristine, cisplatin, methotrexate) treatment display signs of sensory neuropathic pain later in life, typically associated with adolescence (Lu et al., 2011; Ness et al., 2013; Khan et al., 2014). Patients who are diagnosed with cancer in early life (< 10 years old) and are then assessed later in life,

Fig. 11. Cisplatin treatment early in life does not alter sensory neuron number and increases astrocytic activation in the dorsal horn. In P16 age-matched rats that were treated with either cisplatin or vehicle demonstrate no change in [A–B] total neuron number (NeuN) in the dorsal horn. When comparing lamina there were also no differences in [C] total neuron number per laminae. [D–E] Astrocyte (GFAP) number was also unchanged in the dorsal horn in P16 age-matched rats treated with either cisplatin or vehicle. There were no differences in [F] total astrocyte number across lamina I, II and V. In adult (P45) rats treated with cisplatin early in life there were no differences in [G–I] total neuron number (NeuN) across dorsal horn laminae when compared to vehicle-treated age-matched controls. [J–K] There was no change in total astrocyte (GFAP) number, however, there was an increase in lamina V of GFAP-positive astrocytes ($^{*}P < 0.05$ Unpaired t test; vehicle = 5, cisplatin $n = 5$) (scale bar = 100 μm).

present symptoms of CIPN such as hypersensitivity to mechanical stimulation in the hands and arms (Gilchrist and Tanner, 2013; Gilchrist et al., 2014), as well as hallmarks of sensory neurodegeneration (Lu et al., 2011; Khan et al., 2014). These symptoms occur many years after diagnosis and the end of treatment (> 7 yrs) Phillips et al., 2015; Khan et al., 2014. The data presented in this study complement these human studies, whereby early-life treatment with cisplatin leads to the development of neuropathic pain, but this pain does not present until later in life. This delay in the manifestation of neuropathic pain until adulthood when the injury was in early life has been seen with other animal models (McKelvey et al., 2015) and recently presented following early-life exposure to vincristine (Schappacher et al., 2017). It must be noted that acute toxicity and hypersensitivity from chemotherapy exposure has been demonstrated (Joseph and Levine, 2009). In this study acute pain (within hours of drug administration) were not investigated and could be missed. However, heat hypersensitivity develops at a timepoint much later following final cisplatin injections despite regular nociceptive testing. This highlights our primary focus of this study on understanding alterations to the sensory nervous system in adulthood following cisplatin treatment. This further explains our rationale for our chosen methodology for the development of this childhood model of CIPN. Cisplatin administration in humans is typically multiple cycles of treatment (Zsiros et al., 2013) and adult rodent models have been developed to explore CIPN in this setting (Mao-Ying et al., 2014). However, these studies aimed to determine how cisplatin impacts upon sensory neuron development therefore requiring a focussed delivery timeline to allow identification of any nociceptive changes. These data provide the first insight into how cancer treatment can impact upon the developing sensory nervous system and consequently chronic pain in adult childhood cancer survivors.

Cisplatin exposure is associated with long lasting pain

CIPN is long-lasting in adults with pain persisting for many months or years post termination of treatment (Flatters and Bennett, 2006; Paice, 2009; Paice, 2011). Sensory neuronal apoptosis is thought to be restricted to the peripheral nervous system (Jacobs et al., 2010), with neuropathy symptoms typically displayed in the extremities e.g. hands or feet. Targeting of which, can alleviate platinum-based chemotherapy-induced sensory neuropathy (Joseph and Levine, 2009). Despite this obvious impact upon the sensory nervous system particularly in adults and known implications of chemotherapy toxicity to children, minimal information is available on chemotherapy-induced pain in adult childhood cancer survivors. There are increased neurological symptoms in adult childhood cancer patients such as auditory complications (Grewal et al., 2010). Here we present evidence that young animals treated with cisplatin develop a delayed but long lasting pain. The sensory nervous system develops and matures over the first weeks of life; C fiber integration into the spinal dorsal horn and both intrinsic and descending inhibitory tone within the dorsal horn is established (Jennings and Fitzgerald, 1998; Koch et al., 2012), vastly improving motor and sensory acuity (Fitzgerald, 2005). In association neuropathic pain only becomes established 3 weeks postnatally if a traumatic nerve injury is introduced during the initial 2 weeks of life (Vega-Avelaira et al., 2012; McKelvey et al., 2015). Our data demonstrate that cisplatin treatment administered during the second week of life induces neuropathic pain that develops 22 days post-natally. This is highly comparable to studies in pediatric patients whereby pain is uncommon in young children (Walco et al., 2010), however neurological complications and pain are increasingly common in patients with increasing age (Phillips et al., 2015).

Understanding how such chemotherapy treatments impact upon the developing sensory nervous system allows us to design and provide suitable analgesic relief and treatment management to these patients. It is known that if you introduce a noxious insult e.g. traumatic nerve or incisional injury to young individuals that long-lasting pain does not necessarily become apparent until later in life. This has been displayed recently in rats and mice where a spared nerve injury in the first post-natal week led to a delayed hyperalgesia (McKelvey et al., 2015). In addition, this is comparable to human studies where pain does not present until much later in life (Fitzgerald, 2005; Vega-Avelaira et al., 2012; Fitzgerald and McKelvey, 2016). Furthermore, in neonatal animals there is a significant loss of sensory neurons in the initial post-natal weeks (Coggeshall et al., 1994) which is exacerbated following nerve injury (Himes and Tessler, 1989). It has been reported that cisplatin and other platinum-based drugs induce neuronal apoptosis (Gill and Windebank, 1998). However, cisplatin treatment in post-natal week 2 does not lead to alterations in DRG neuronal number or sub-classifications in the immature (P16) tissue but demonstrates increases in neuronal

stress presented by increases in cleaved caspase III when compared to the vehicle group in the immature group. Interestingly the tissue extracted from adult (P45) rats treated with cisplatin also do not display any difference in DRG number or alterations in DRG neuron soma size compared to vehicle control animals therefore cisplatin-induced sensory neuropathy is not associated with neuronal apoptosis in this instance. However, following a traumatic nerve injury, sensory DRG neurons have the capability to regenerate, hyperinnervating peripheral and central targets (Himes and Tessler, 1989; Shortland and Fitzgerald, 1994). There can be expansive remodeling of peripheral nerve innervation patterns in the skin (Reynolds and Fitzgerald, 1995) as well as into the dorsal horn of the spinal cord (Shortland and Fitzgerald, 1994); which is typified by a spike in nerve growth factor expression in neonatal and adult rodents (Lewin and Mendell, 1994; Constantinou et al., 1994). Cisplatin treatment in the second post-natal week led to striking a hyperinnervation in adults, with an increased IENF into the plantar skin of CGRP + ve and PGP9.5 + ve nerve fibers. This is accompanied by alterations in the innervation pattern of the sensory afferent central terminals with elevated levels and/or alterations in depth of lamina innervation displayed by C fibers and A fibers. As mentioned sensory axonal and nerve fiber processes do have the ability to recover following chemotherapy treatment (Flatters and Bennett, 2006), however such chemotherapy treatments potentially initiates aberrant growth of sensory nerve fibers due to the impact on developing tissues as highlighted whereby NGF is administered in neonatal peripheral tissues (Lewin and Mendell, 1994; Constantinou et al., 1994). This is in contrast to earlier timepoints where IENF innervation is reduced following cisplatin treatment. It is known that the sensory nerve can regenerate following an insult (Ma et al., 2011) and that treatment or disease induces uncontrolled aberrant sensory nerve fiber growth, to which is associated with chronic pain development such as in rodent models of arthritis (Ghilardi et al., 2012) and cancer pain (Bloom et al., 2011). We postulate here that despite initial suppression of the regenerative capacity (decrease in ATF3 expression (Vencappa et al., 2015) following cisplatin exposure, endogenous regenerative mechanisms are induced driving this aberrant growth. Further understanding of these mechanisms is needed to allow us to potentially identify key mechanisms associated with chronic pain development.

Changes in C fiber innervation patterns peripherally and centrally we believe could be attributable to the delayed but long-lasting pain induced by cisplatin. Furthermore, the onset of mechanical and heat hyperalgesia can be associated with the onset of C fiber sensitization (Djouhri et al., 2001; Djouhri et al., 2006; Hulse et al., 2010; Hulse, 2016). This can be prevented through the inhibition of the NGF-TrkA axis (Djouhri et al., 2001). It is plausible that cisplatin-induced survivorship pain is mediated by TrkA-dependent mechanisms, which is widely acknowledged as a key component of sensory neuron trophic support and chronic pain development (Bloom et al., 2011; Ghilardi et al., 2012). Induction

of NGF-TrkA signaling is highly plausible as the percentage of sensory DRG neurons expressing TrkA (tropomysin receptor kinase A) as well as dorsal horn innervation of TrkA-positive sensory afferent terminals were upregulated in the cisplatin adult (P45) group versus vehicle age-matched controls. Aberrant branching of sensory nociceptors has been widely associated with the development of hyperalgesia and peripheral sensory nerve sensitization typically associated with disease such as arthritis (Jimenez-Andrade and Mantyh, 2012) and bone cancer (Jimenez-Andrade et al., 2010; Bloom et al., 2011). With regards to A fiber function; A fiber sensitization has been associated with onset of chronic pain (Tsantoulas et al., 2012) and that A fiber sensitization occurs comparably in inflammatory arthritis in both hairy and glabrous skin (Drake et al., 2014). However, our conclusions as regards delayed onset of chronic pain need to also consider that descending control can impact upon nociceptive processing with regards to A fiber inputs, to the instance that A fiber induced chronic pain can be blocked via activation of inhibitory descending modulation (Drake et al., 2014). This is in addition to decreased A fiber innervation into the hairy surface of the hindpaw which would lead to reduced sensory dexterity (Boada et al., 2010). Therefore delayed mechanical allodynia in this instance could be due to inhibitory descending control or alternatively due to lack of sensitization on the hairy side of the hindpaw.

CIPN is a common complaint of adults receiving chemotherapy, especially cisplatin, in addition to the inability to sleep, low mood and difficulty performing everyday tasks. It is important in clinical practice to understand the long-term effects of chemotherapy on children and the developing nervous system. Childhood cancer survivors appear to have a delayed onset of neuropathic pain compared to adults for whom there is an immediate onset of allodynia and hyperalgesia. Plasticity in the immature nervous system and impact of cisplatin treatment leads to the normal development of nociceptive pathways being disrupted. A change in pain processing due to chemotherapy treatment, manifesting as hypersensitivity, could impact patient quality of life. Few studies, however, have documented the late effects of chemotherapeutic agents in pediatric patients or the future impact of CIPN. Hence, the hyperalgesia observed here holds clinical importance with many patients experiencing late effects of their treatment. Clinically, an intervention which prevents abnormal maturation yet provides symptom relief may be viable in the future.

REFERENCES

Bloom AP, Jimenez-Andrade JM, Taylor RN, Castaneda-Corral G, Kaczmarska MJ, Freeman KT, et al. (2011) Breast cancer-induced bone remodeling, skeletal pain, and sprouting of sensory nerve fibers. J Pain 12(6):698–711.

Boada MD, Houle TT, Eisenach JC, Ririe DG (2010) Differing neurophysiologic mechanosensory input from glabrous and hairy skin in juvenile rats. J Neurophysiol 104(6):3568–3575.

Clanton NR, Klosky JL, Li C, Jain N, Srivastava DK, Mulrooney D, et al. (2011) Fatigue, vitality, sleep, and neurocognitive functioning in adult survivors of childhood cancer: a report from the Childhood Cancer Survivor Study. Cancer 117 (11):2559–2568.

Coggeshall RE, Pover CM, Fitzgerald M (1994) Dorsal root ganglion cell death and surviving cell numbers in relation to the development of sensory innervation in the rat hindlimb. Brain Res Dev Brain Res 82(1–2):193–212.

Constantinou J, Reynolds ML, Woolf CJ, Safieh-Garabedian B, Fitzgerald M (1994) Nerve growth factor levels in developing rat skin: upregulation following skin wounding. NeuroReport 5 (17):2281–2284.

Djouhri LDD, Robertson A, Newton R, Lawson SN (2001) Time course and nerve growth factor dependence of inflammation-induced alterations in electrophysiological membrane properties in nociceptive primary afferent neurons. J Neurosci 21 (22):8722–8733.

Djouhri L, Koutsikou S, Fang X, McMullan S, Lawson SN (2006) Spontaneous pain, both neuropathic and inflammatory, is related to frequency of spontaneous firing in intact C-fiber nociceptors. J Neurosci 26(4):1281–1292.

Drake R, Hulse R, Lumb B, Donaldson L (2014) The degree of acute descending control of spinal nociception in an area of primary hyperalgesia is dependent on the peripheral domain of afferent input. J Physiol 592(16):3611–3624.

Fitzgerald M (2005) The development of nociceptive circuits. Nat Rev Neurosci 6(7):507–520.

Fitzgerald M, McKelvey R (2016) Nerve injury and neuropathic pain – a question of age. Exp Neurol 275(Pt 2):296–302.

Flatters SJ, Bennett GJ (2006) Studies of peripheral sensory nerves in paclitaxel-induced painful peripheral neuropathy: evidence for mitochondrial dysfunction. Pain 122(3):245–257.

Ghilardi JR, Freeman KT, Jimenez-Andrade JM, Coughlin KA, Kaczmarska MJ, Castaneda-Corral G, et al. (2012) Neuroplasticity of sensory and sympathetic nerve fibers in a mouse model of a painful arthritic joint. Arthritis Rheum 64 (7):2223–2232.

Gilchrist LS, Tanner L (2013) The pediatric-modified total neuropathy score: a reliable and valid measure of chemotherapy-induced peripheral neuropathy in children with non-CNS cancers. Support Care Cancer 21(3):847–856.

Gilchrist LS, Marais L, Tanner L (2014) Comparison of two chemotherapy-induced peripheral neuropathy measurement approaches in children. Support Care Cancer 22(2):359–366.

Giles PA, Trezise DJ, King AE (2007) Differential activation of protein kinases in the dorsal horn in vitro of normal and inflamed rats by group I metabotropic glutamate receptor subtypes. Neuropharmacology 53(1):58–70.

Gill JS, Windebank AJ (1998) Cisplatin-induced apoptosis in rat dorsal root ganglion neurons is associated with attempted entry into the cell cycle. J Clin Investig 101(12):2842–2850.

Grewal S, Merchant T, Reymond R, McInerney M, Hodge C, Shearer P (2010) Auditory late effects of childhood cancer therapy: a report from the Children's Oncology Group. Pediatrics 125(4): e938–e950.

Himes BT, Tessler A (1989) Death of some dorsal root ganglion neurons and plasticity of others following sciatic nerve section in adult and neonatal rats. J Comp Neurol 284(2):215–230.

Hulse RP (2016) Identification of mechano-sensitive C fibre sensitization and contribution to nerve injury-induced mechanical hyperalgesia. Eur J Pain 20(4):615–625.

Hulse R, Wynick D, Donaldson L (2010) Intact cutaneous C fibre afferent properties in mechanical and cold neuropathic allodynia. Eur J Pain 14(6):565.

Hulse RP, Beazley-Long N, Ved N, Bestall SM, Riaz H, Singhal P, et al. (2015) Vascular endothelial growth factor-A165b prevents diabetic neuropathic pain and sensory neuronal degeneration. Clin Sci 129(8):741–756.

Jacobs S, McCully CL, Murphy RF, Bacher J, Balis FM, Fox E (2010) Extracellular fluid concentrations of cisplatin, carboplatin, and oxaliplatin in brain, muscle, and blood measured using microdialysis in nonhuman primates. Cancer Chemother Pharmacol 65(5):817–824.

Jennings E, Fitzgerald M (1998) Postnatal changes in responses of rat dorsal horn cells to afferent stimulation: a fibre-induced sensitization. J Physiol 509(Pt 3):859–868.

Jimenez-Andrade JM, Mantyh PW (2012) Sensory and sympathetic nerve fibers undergo sprouting and neuroma formation in the painful arthritic joint of geriatric mice. Arthritis Res Ther 14(3): R101.

Jimenez-Andrade JM, Bloom AP, Stake JI, Mantyh WG, Taylor RN, Freeman KT, et al. (2010) Pathological sprouting of adult nociceptors in chronic prostate cancer-induced bone pain. J Neurosci 30(44):14649–14656.

Jin HW, Flatters SJ, Xiao WH, Mulhern HL, Bennett GJ (2008) Prevention of paclitaxel-evoked painful peripheral neuropathy by acetyl-L-carnitine: effects on axonal mitochondria, sensory nerve fiber terminal arbors, and cutaneous Langerhans cells. Exp Neurol 210(1):229–237.

Joseph E, Levine J (2009) Comparison of oxaliplatin- and cisplatin-induced painful peripheral neuropathy in the rat. J Pain 10 (5):534–541.

Khan R, Hudson M, Ledet D, Morris E, Pui C, Howard S, et al. (2014) Neurologic morbidity and quality of life in survivors of childhood acute lymphoblastic leukemia: a prospective cross-sectional study. J Cancer Surviv 8(4):688–696.

Koch SC, Tochiki KK, Hirschberg S, Fitzgerald M (2012) C-fiber activity-dependent maturation of glycinergic inhibition in the spinal dorsal horn of the postnatal rat. PNAS 109(30):12201–12206.

Kunin-Batson AS, Lu X, Balsamo L, Graber K, Devidas M, Hunger SP, et al. (2016) Prevalence and predictors of anxiety and depression after completion of chemotherapy for childhood acute lymphoblastic leukemia: a prospective longitudinal study. Cancer 122(10):1608–1617.

Lewin GR, Mendell LM (1994) Regulation of cutaneous C-fiber heat nociceptors by nerve growth factor in the developing rat. J Neurophysiol 71(3):941–949.

Lorenzo L-E, Ramien M, St Louis M, De Koninck Y, Ribeiro-Da-Silva A (2008) Postnatal changes in the rexed lamination and markers of nociceptive afferents in the superficial dorsal horn of the rat. J Comp Neurol 592–604.

Lu Q, Krull KR, Leisenring W, Owen JE, Kawashima T, Tsao JC, et al. (2011) Pain in long-term adult survivors of childhood cancers and their siblings: a report from the Childhood Cancer Survivor Study. Pain 152(11):2616–2624.

Ma CH, Omura T, Cobos EJ, Latremoliere A, Ghasemlou N, Brenner GJ, et al. (2011) Accelerating axonal growth promotes motor recovery after peripheral nerve injury in mice. J Clin Investig 121 (11):4332–4347.

Mao-Ying QL, Kavelaars A, Krukowski K, Huo XJ, Zhou W, Price TJ, et al. (2014) The anti-diabetic drug metformin protects against chemotherapy-induced peripheral neuropathy in a mouse model. PLoS ONE 9(6):e100701.

McKelvey R, Berta T, Old E, Ji R, Fitzgerald M (2015) Neuropathic pain is constitutively suppressed in early life by anti-inflammatory neuroimmune regulation. J Neurosci 35(2):457–466.

McWhinney SR, Goldberg RM, McLeod HL (2009) Platinum neurotoxicity pharmacogenetics. Mol Cancer Ther 8(1):10–16.

Ness K, Jones K, Smith W, Spunt S, Wilson C, Armstrong G, et al. (2013) Chemotherapy-related neuropathic symptoms and functional impairment in adult survivors of extracranial solid tumors of childhood: results from the St. Jude Lifetime Cohort Study. Arch Phys Med Rehabil 94(8):1451–1457.

Paice J (2009) Clinical challenges: chemotherapy-induced peripheral neuropathy. Semin Oncol Nurs 25(2). S8-19.

Paice JA (2011) Chronic treatment-related pain in cancer survivors. Pain 152(3 Suppl). S84-9.

Park H, Stokes J, Pirie E, Skahen J, Shtaerman Y, Yaksh T (2013) Persistent hyperalgesia in the cisplatin-treated mouse as defined by threshold measures, the conditioned place preference paradigm, and changes in dorsal root ganglia activated transcription factor 3: the effects of gabapentin, ketorolac, and etanercept. Anesth Analg 116(1):224–231.

Park SB, Goldstein D, Krishnan AV, Lin CS, Friedlander ML, Cassidy J, et al. (2013) Chemotherapy-induced peripheral neurotoxicity: a critical analysis. CA Cancer J Clin 63(6):419–437.

Phillips SM, Padgett LS, Leisenring WM, Stratton KK, Bishop K, Krull KR, et al. (2015) Survivors of childhood cancer in the united states: prevalence and burden of morbidity. Cancer Epidemiol Biomark Prev 24(4):653–663.

Reynolds ML, Fitzgerald M (1995) Long-term sensory hyperinnervation following neonatal skin wounds. J Comp Neurol 358(4):487–498.

Schappacher KA, Styczynski L, Baccei ML (2017) Early life vincristine exposure evokes mechanical pain hypersensitivity in the developing rat. Pain 158(9):1647–1655.

Seretny M, Currie GL, Sena ES, Ramnarine S, Grant R, MacLeod MR, et al. (2014) Incidence, prevalence, and predictors of chemotherapy-induced peripheral neuropathy: a systematic review and meta-analysis. Pain 155(12):2461–2470.

Shortland P, Fitzgerald M (1994) Neonatal sciatic nerve section results in a rearrangement of the central terminals of saphenous and axotomized sciatic nerve afferents in the dorsal horn of the spinal cord of the adult rat. Eur J Neurosci 6(1):75–86.

Smith MA, Seibel NL, Altekruse SF, Ries LA, Melbert DL, O'Leary M, et al. (2010) Outcomes for children and adolescents with cancer: challenges for the twenty-first century. J Clin Oncol 28 (15):2625–2634.

Ta LE, Espeset L, Podratz J, Windebank AJ (2006) Neurotoxicity of oxaliplatin and cisplatin for dorsal root ganglion neurons correlates with platinum-DNA binding. Neurotoxicology 27 (6):992–1002.

Thakur M, Rahman W, Hobbs C, Dickenson AH, Bennett DL (2012) Characterisation of a peripheral neuropathic component of the rat monoiodoacetate model of osteoarthritis. PLoS ONE 7(3): e33730.

Tsantoulas C, Zhu L, Shaifta Y, Grist J, Ward JP, Raouf R, et al. (2012) Sensory neuron downregulation of the Kv9.1 potassium channel subunit mediates neuropathic pain following nerve injury. J Neurosci 32(48):17502–17513.

Uhelski ML, Khasabova IA, Simone DA (2015) Inhibition of anandamide hydrolysis attenuates nociceptor sensitization in a murine model of chemotherapy-induced peripheral neuropathy. J Neurophysiol 113(5):1501–1510.

van As JW, van den Berg H, van Dalen EC (2012) Medical interventions for the prevention of platinum-induced hearing loss in children with cancer. Cochrane Database Syst Rev 5:1. CD009219.

Vega-Avelaira D, McKelvey R, Hathway G, Fitzgerald M (2012) The emergence of adolescent onset pain hypersensitivity following neonatal nerve injury. Mol Pain 8(30).

Vencappa S, Donaldson LF, Hulse RP (2015) Cisplatin induced sensory neuropathy is prevented by vascular endothelial growth factor-A. Am J Transl Res 7(6):1032–1044.

Walco GA, Dworkin RH, Krane EJ, LeBel AA, Treede RD (2010) Neuropathic pain in children: special considerations. Mayo Clin Proc 85(3 Suppl):S33–S41.

Ward E, DeSantis C, Robbins A, Kohler B, Jemal A (2014) Childhood and adolescent cancer statistics, 2014. CA Cancer J Clin 64 (2):83–103.

Zsiros J, Maibach R, Shafford E, Brugieres L, Brock P, Czauderna P, et al. (2010) Successful treatment of childhood high-risk

hepatoblastoma with dose-intensive multiagent chemotherapy and surgery: final results of the SIOPEL-3HR study. J Clin Oncol 28(15):2584–2590.

Zsiros J, Brugieres L, Brock P, Roebuck D, Maibach R, Zimmermann A, et al. (2013) Dose-dense cisplatin-based chemotherapy and surgery for children with high-risk hepatoblastoma (SIOPEL-4): a prospective, single-arm, feasibility study. Lancet Oncol 14 (9):834–842.